Journal of Environmental Management 336 (2023) 117655

Contents lists available at ScienceDirect

Journal of Environmental Management

journal homepage: www.elsevier.com/locate/jenvman

Research article

Browning of vegetation in efficient carbon sink regions of India during the past two decades is driven by climate change and anthropogenic intrusions

Rahul Kashyap, Jayanarayanan Kuttippurath *, Pankaj Kumar

CORAL, Indian Institute of Technology Kharagpur, Kharagpur, 721302, India

ARTICLE INFO

Keywords:
Carbon use efficiency (CUE)
Vegetation carbon dynamics (VCD)
Land-atmosphere interactions
Carbon cycle
Principal component analyses (PCA)
Causal discovery

ABSTRACT

Accurate estimation of carbon cycle is a challenging task owing to the complexity and heterogeneity of ecosystems. Carbon Use Efficiency (CUE) is a metric to define the ability of vegetation to sequester carbon from the atmosphere. It is key to understand the carbon sink and source pathways of ecosystems. Here, we quantify CUE using remote sensing measurements to examine its variability, drivers and underlying mechanisms in India for the period 2000–2019, by applying the principal component analyses (PCA), multiple linear regression (MLR) and causal discovery. Our analysis shows that the forests in the hilly regions (HR) and northeast (NE), and croplands in the western areas of South India (SI) exhibit high (>0.6) CUE. The northwest (NW), Indo-Gangetic plain (IGP) and some areas in Central India (CI) show low (<0.3) CUE. In general, the water availability as soil moisture (SM) and precipitation (P) promote higher CUE, but higher temperature (T) and air organic carbon content (AOCC) reduce CUE. It is found that SM has the strongest relative influence (33%) on CUE, followed by P. Also, SM has a direct causal link with all drivers and CUE; reiterating its importance in driving vegetation carbon dynamics (VCD) for the cropland dominated India. The long-term analysis reveals that the low CUE regions in NW (moisture induced greening) and IGP (irrigation induced agricultural boom) have an increasing trend in productivity (greening). However, the high CUE regions in NE (deforestation and extreme events) and SI (warming induced moisture stress) exhibit a decreasing trend in productivity (browning), which is a great concern. Our study, therefore, provides new insights on the rate of carbon allocation and the need of proper planning for maintaining balance in the terrestrial carbon cycle. This is particularly important in the context of drafting policy decisions for the mitigation of climate change, food security and sustainability.

1. Introduction

Human perturbations have led to highly capricious response of terrestrial vegetation to the changes in climate (Newbold et al., 2020). Modifications in the fluxes of momentum, water and energy in the earth system between land surface and atmosphere in recent decades have triggered significant variability in vegetation carbon dynamics (VCD) (He et al., 2018; Gang et al., 2022). Climate change has emerged as the most important and unpredictable factor that influences VCD. The scenario of limited water due to lower precipitation and warming of both atmosphere and land can decline terrestrial productivity (Gahlot et al., 2017; IPCC, 2019). Along with the changes in climate, various anthropogenic influences such as land use land cover change (LULCC), agricultural production and irrigation impacts VCD (Nemani et al., 2003; Chen et al., 2019).

Vegetation greening has a significant role in mitigation of global warming and climate change, because the terrestrial vegetation acts as a major carbon sink (Piao et al., 2020; Sarmah et al., 2021). South Asia has been greening in the last two decades (Parida et al., 2020; Kashyap et al., 2022) and much of it is contributed by India and China (Chen et al., 2019). However, quantification of this greening in terms of terrestrial carbon sequestration is largely unknown (Sarmah et al., 2021; Verma et al., 2022). The carbon cycle will be strongly impacted by the regional climate change in south Asia, and India is a region yet to be adequately explored with respect to carbon budget studies (Bala et al., 2013; Sarmah et al., 2021; Verma et al., 2022). Scarcity of data, extensive computational requirements and the complex land-atmosphere interactions in Indian region pose great challenges for undertaking such studies (Sarmah et al., 2021; Verma et al., 2022).

Carbon use efficiency (CUE) is a measure of the ability of vegetation to sequester atmospheric carbon and is estimated as the ratio of Net primary productivity (NPP) to Gross primary productivity (GPP) (De

* Corresponding author.
E-mail address: jayan@coral.iitkgp.ac.in (J. Kuttippurath).

https://doi.org/10.1016/j.jenvman.2023.117655
Received 2 November 2022; Received in revised form 25 February 2023; Accepted 1 March 2023
Available online 8 March 2023
0301-4797/© 2023 Elsevier Ltd. All rights reserved.

Lucia et al., 2007). It gives the amount of carbon stored and used for growth out of the net carbon acquired by the ecosystem. CUE provides insight on the vegetation functioning as it is the rate of conversion of GPP to NPP or the splitting of GPP to NPP and autotrophic respiration (Ra) (He et al., 2018; Gang et al., 2022). Although it is a simple method as per concept, the estimation of CUE requires measurement of carbon uptake and its use for the growth, which makes it computationally very challenging (Migliavacca et al., 2021; Gang et al., 2022). GPP and NPP are the most important ecosystem variables that are studied extensively, as they are the fundamental ecological variables, which quantify the terrestrial carbon assimilation (Nemani et al., 2003; Bala et al., 2013). GPP is the rate of carbon dioxide captured by vegetation in a given period of time through photosynthesis. NPP is the residual of GPP after Ra, and is measured as the net production or accumulation of dry organic matter in vegetation (Roxburgh et al., 2005; Ballantyne et al., 2012). Terrestrial ecosystem carbon sink estimates, natural resource management and ecological studies are challenged by the high spatio-temporal variability of productivity (Ballantyne et al., 2012; Sarmah et al., 2021).

Direct measurement of GPP and NPP based on instruments at landscape, ecosystem and canopy level is still a daunting task. Therefore, quantification of global productivity highly relies on remote sensing measurements from space and model simulations (Ballantyne et al., 2012; Garbulsky et al., 2014). Satellite remote sensing enables larger sample size with unmatched global measurements for the synoptic monitoring of biosphere (Bala et al., 2013; Chen et al., 2019; Kashyap et al., 2022). Moreover, the unavailability of flux tower measurements in the regions of high carbon uptake makes remote sensing based VCD estimation inevitable (Sarmah et al., 2021; Verma et al., 2022).

Terrestrial carbon budgeting is vital for understanding of the land-atmosphere interactions, carbon sequestration, biosphere-climate feedback and climate change mitigation (Campbell et al., 2017; Newbold et al., 2020). We hypothesise that, VCD regulate the functioning of terrestrial ecosystems including carbon capture (GPP), storage (NPP) and rate of storage (CUE), and is influenced by certain drivers such as the fraction of photosynthetically active radiation (FPAR), temperature (T), precipitation (P), soil moisture (SM) and air organic carbon content (AOCC). Evaluation of CUE, its drivers and the underlying mechanisms are key to understand the terrestrial carbon cycle. It provides a better understanding of the changes in climate, and energy exchange between vegetation and atmosphere. Our study considers algorithms such as principal component analysis (PCA, rotated and unrotated), multiple linear regression (MLR) and causal discovery for understanding the drivers of CUE in India. This is the first of its kind analysis on CUE and its drivers in the Indian context and is the significance of this study.

2. Data and methodology

2.1. Data

The suitability and efficiency of Moderate Resolution Imaging Spectroradiometer (MODIS) data for studying large-scale terrestrial ecosystems are well established (e.g. Chen et al., 2019; Sarmah et al., 2021; Kashyap et al., 2022). MODIS GPP (MOD 17 A2HGF) and NPP (MOD 17 A3HGF) primary productivity data are considered here (Turner et al., 2006; Running et al., 2015). The Vegetation Index (VI) data taken are the MODIS based (MOD13A1) Normalised Difference Vegetation Index (NDVI) (e.g., Liu et al., 2017; Singh et al., 2022). The MCD12Q1 version 6 data provide land cover types using supervised classification. The land temperature (T) data are from the Global Land Data Assimilation System (GLDAS) NOAH 025 M 21 that are a blend of National Ocean and Atmospheric Administration and Global Data Assimilation System (NOAA/GDAS) atmospheric analysis (Wang et al., 2016; Xia et al., 2019). The precipitation (P) data are from the Global Precipitation Measurements (GPM, GPM_3IMERGDF L3), which is a multi-satellite integrated precipitation dataset with daily (mm/day) accumulated values (Xu et al., 2017). The GLDAS-based soil moisture data (SM) are also utilised in the study (Liu et al., 2019). The Modern Era Retrospective analysis for Research and Applications Version 2 (MERRA–2) air organic carbon content (AOCC) data are used for the atmospheric organic carbon estimates (Shikwambana, 2019), as listed in Table 1.

2.2. Methodology

2.2.1. Estimation of variability in productivity and CUE

This study is conducted for the Indian land region as shown in Fig. S1 and Table S1. The MODIS land cover data are used to mask the vegetated land comprising of forests and croplands. The MODIS GPP and NPP are based on the rate of dry matter formation from absorbed radiation, called the light use efficiency (LUE) model approach. This is the most commonly used method for productivity computation using remote sensing measurements (Wang et al., 2017; Sarmah et al., 2021; Verma et al., 2022). The MODIS-based gap-filled GPP data for winter (December, January, and February – DJF), summer (March, April, and May – MAM), monsoon (June, July, and August – JJA) and post-monsoon (September, October, and November – SON) seasons over the years 2000–2019 are averaged to obtain the respective seasonal means. However, the NPP data are considered only for the yearly and decadal averages, as there are no seasonal data. The trend in GPP is computed for three focal periods: study period (2000–2019), previous decade (2000–2009) and recent decade (2010–2019). The negative trend in productivity is called browning and positive trend is greening. The spatio-temporal analyses of CUE, its drivers and their temporal trends are also computed. Since, the NPP data are available in the yearly frequency, we estimated the seasonality/seasonal anomaly (Si, i for each season) in GPP as the departure from the mean in each season (Xi) from the annual mean (X). That is, $Si = X - Xi$. Since our analysis focuses on the seasonal VCD, we did not consider smaller temporal scales. Based on the seasonality in GPP, the seasonal variation in NPP and CUE are estimated. CUE is estimated as the ratio of NPP to GPP (De Lucia et al., 2007).

2.2.2. Connection, contribution and influence of drivers

PCA has been widely used in climate science for teleconnection analyses (Lim, 2015; Gao et al., 2017; Mezzina et al., 2020). To better understand the linkages among the drivers and CUE, we have performed both unrotated (UPCA) and rotated PCA (RPCA) in our analysis. The method is detailed in supplementary file. However, it should be noted

Table 1
Datasets with their resolution, purpose they serve in this study and source from which they are acquired.

Data Used	Resolution	Purpose	Source
MODIS NDVI	500 m	NDVI used for estimating FPAR	(https://lpdaacsvc.cr.usgs.gov/)
MODIS GPP	500 m	GPP, GPP trend, CUE estimation	(https://lpdaacsvc.cr.usgs.gov/)
MODIS NPP	500 m	NPP, CUE estimation	(https://lpdaacsvc.cr.usgs.gov/)
MODIS Land Cover	500 m	LULC data to extract vegetated land comprising of forests and croplands	(https://lpdaacsvc.cr.usgs.gov/)
GPM Level-3 precipitation	0.1° × 0.1°	Precipitation, relationship with CUE	(https://daac.gsfc.nasa.gov/)
GLDAS Temperature	0.25° × 0.25°	Temperature, relationship with CUE	(https://daac.gsfc.nasa.gov/)
MERRA– 2 Air organic carbon	0.5° × 0.625°	Air organic carbon, relationship with CUE	(https://daac.gsfc.nasa.gov/)
GLDAS Soil Moisture	0.25 × 0.25°	Soil Moisture, relationship with CUE	(https://daac.gsfc.nasa.gov/)

that relationship between PCA output and physical processes is not straightforward (Spensberger et al., 2020).

The relative contribution and influence of drivers to productivity (P) and CUE variability are estimated using the modified multiple linear region (MLR, Kashyap et al., 2022) where the normalised trend (trend/range) is used in place of trend unlike the conventional MLR (e.g. Kuttippurath and Nair, 2017; Kuttippurath et al., 2021) as detailed in supplementary file.

2.2.3. Causal discovery of drivers

Sensitivity of ecological systems and their interactions with both climate and anthropogenic processes have a nonlinear relationship and is very complex (Gahlot et al., 2017). Correlation is insufficient for detecting the complex and nonlinear associations with drivers with substantial autocorrelation, which does not necessarily imply causation (Runge et al., 2019). True causality necessitates not just the establishment of relationship among the variables, but also provides its direction (e.g. Kumar et al., 2022). This study uses one such causal model within Pearl Causality (PC) framework to discover the potential drivers of CUE and PCMCI is the most widely used algorithm in climate science for causal discovery (e.g. Krich et al., 2020; Verma et al., 2022).

In the first stage, the PCMCI algorithm identifies each driver's parents by performing an iterative conditional independence test by calculating the partial correlation between two time series. In the second stage, it assesses the statistical significance of causal links using momentary conditional independence (MCI) tests, and then estimates the strength of causal links using multiple linear regression (MLR). To determine causality, the PCMCI method employs a number of statistical tests, including linear partial correlations (Par-Corr) and nonlinear independence tests such as Gaussian process regressions and distance correlation (GPDC) and conditional mutual information (CMI). The PCMCI algorithm has two free parameters that the user must choose: maximum time delay (T_{max}) and significance threshold (ά), which define the acceptable level of false-positive link discovery. For identifying causal links, this study employs PCMCI+ (a PCMCI extension) to allow the discovery of contemporaneous links based on linear Par-corr tests (Muñoz et al., 2021). Kwiatkowski-Phillips-Schmidt-Shin (KPSS) test and the Augmented Dickey-Fuller (ADF) unit root test are used to examine the stationarity of the dataset prior to the causal analysis.

3. Results

3.1. Seasonal and decadal variability in terrestrial productivity

The average GPP in various seasons for India during the period 2000–2019 is shown in Fig. 1. In winter, high (>250 gC/m^2/yr) GPP in Punjab and Haryana and moderate GPP (100–250 gC/m^2/yr) in the rest of Indo-Gangetic plain (IGP) are observed. This is due to the rabi agriculture in this season, which is supported by optimum T (15–20 °C) and moderate SM (50–75 kg/m^2) that lead to higher (>0.7) FPAR there, as shown in Figs. S2 and S3. In summer, majority of the lands show lower GPP (<100 gC/m^2/yr) due to little P (<0.5 mm/day), lower SM (<75 kg/m^2), moderate FPAR (0.4–0.6) and very high AOCC (>20 mg/m^2). In monsoon, NE (>500 gC/m^2/yr), CI, and the western and eastern Ghats exhibit high GPP (>250 gC/m^2/yr) owing to higher P (>7.5 mm/day) and SM (>125 kg/m^2). However, higher T (>30 °C), lower SM (50–75 kg/m^2) and high AOCC (15–20 mg/m^2) lead to moderate (100–250 gC/m^2/yr) GPP in NW, IGP and some areas in SI. In post-monsoon, NE (>500 gC/m^2/yr), the eastern coasts and SI show higher GPP (>250 gC/m^2/yr) because of relatively high P (>5 mm/day) and SM (>125 kg/m^2)

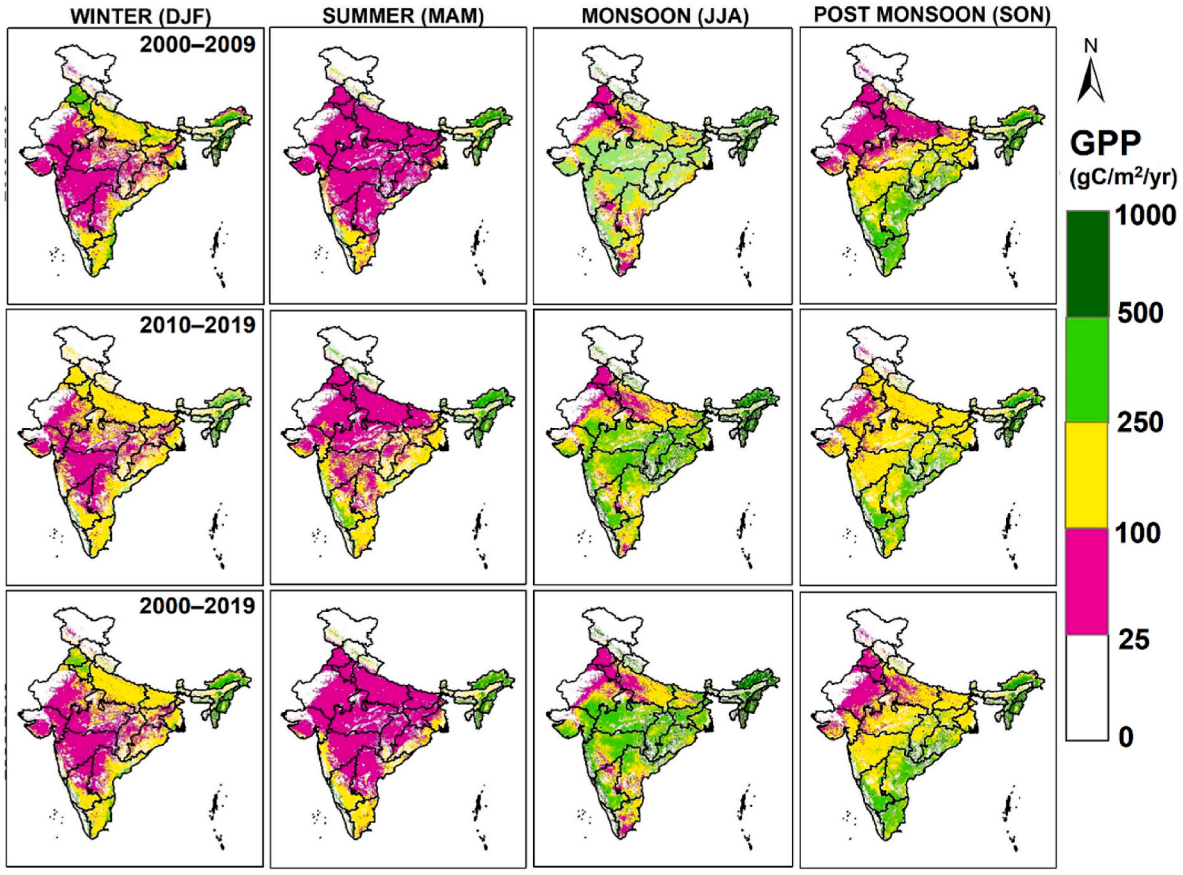

Fig. 1. Gross Primary Productivity (GPP) during winter (December, January and February), summer (March, April and May), monsoon (June, July and August) and post–monsoon (September, October and November) seasons for the period 2000–2009 (top panel), 2010–2019 (middle panel) and 2000–2019 (bottom panel).

there.

The spatio-temporal variability in terrestrial primary productivity i.e. GPP (Fig. 1) and NPP (Fig. 2) for both focal periods: (i) previous decade (2000–2009) and (ii) recent decade (2010–2019) are also estimated. In winter, NW and IGP (Punjab and Haryana) depict enhanced GPP, but it is lower in the northern SI for recent decade in comparison to the previous decade. During summer, GPP is lower in NE and higher in the western areas of SI in recent decade. In monsoon and post-monsoon seasons, majority of the regions exhibits an increase in GPP in recent decade, except in SI. The NPP for the period 2000–2019 exhibits a specific spatial pattern in India, as illustrated in Fig. 2. For instance, high (>200 gC/m^2/yr) NPP is observed in the forest areas of HR (western Himalaya) and NE. Croplands, mainly in CI and SI, also exhibit high NPP. In previous decade, NW and some areas in IGP exhibited lower NPP (<100 gC/m^2/yr), whereas NE, coastal areas, SI and some regions in IGP show higher NPP (>200 gC/m^2/yr). Interestingly, the western Himalaya, IGP, CI and northern SI show an increase in NPP in recent decade. Similar, results are also observed for GPP, with a strong increase in NW and IGP, but a substantial reduction in NE and SI regions.

3.2. Carbon Use Efficiency (CUE) of vegetation

3.2.1. Seasonal variability in CUE

The seasonal variability of CUE in the vegetated Indian landmass for the period 2000–2019 is illustrated in Fig. 3. In winter, the colder regions (5–10 °C) of NW with little P (0–0.5 mm/day) show very small (0.15–0.3) CUE (Figs. S2 and S3). Most areas in IGP, CI and some areas in SI with limited P (0–0.5 mm/day) and SM (50–75 kg/m^2) exhibit moderate (0.3–0.45) CUE. On the contrary, the croplands in SI with optimum T (10–20 °C) and moderate SM (50–75 kg/m^2) promote higher (0.6–0.75) CUE there. The forests in the western Himalaya with higher P (2.5–5 mm/day) and very small AOCC (5–15 mg/m^2) show the highest (0.75–0.9) CUE among the regions. During summer, limited P (0.5–2.5 mm/day) and SM (25–50 kg/m^2) with high T (30–40 °C) and AOCC (25–35 mg/m^2) lead to very small (0.15–0.3) CUE in some areas of IGP and NW. The availability of moisture in terms of P (0.5–2.5 mm/day) and SM (50–100 kg/m^2) outplays the warm summer conditions (30–40 °C) to produce moderate (0.3–0.45) CUE in most areas of CI and SI. Conversely, the low T (5–15 °C), high P (2.5–7.5 mm/day) and moderate AOCC (15–25 mg/m^2) in the Himalaya results in very high (0.75–0.9) CUE in these regions.

In monsoon season, northern IGP with lower SM (25–50 kg/m^2) show very small (0.15–0.3) CUE. Although there is high T (30–40 °C), the water availability in terms of both P (2.5–5 mm/day) and SM (75–125 kg/m^2) results in higher (0.45–0.6) CUE in SI. Some coastal regions experience higher P (7.5–30 mm/day) that promote high (0.6–0.75) CUE there. Very high SM (>100 kg/m^2) in the western areas of SI promote higher CUE (>0.6) in both monsoon and post-monsoon seasons. The eastern Himalaya has this cultivation season supported by sufficient P (15–30 mm/day) and SM (75–100 kg/m^2) lead to high CUE in those regions. During post-monsoon, limited SM (50–75 kg/m^2) in northern IGP produce low (0.15–0.3) CUE. Favourable P (2.5–5 mm/day) and SM (75–125 kg/m^2) promote high (0.45–0.75) CUE in CI. Forests in HR (western Himalaya) with high P (5–30 mm/day) and lower T (5–15 °C) lead to very high (0.75–0.9) CUE in the region. The spatial variability in CUE is in accordance with that of GPP and NPP, and with its drivers in each region. Henceforth, there exists a close link between CUE and GPP-NPP variability.

3.2.2. Vegetation carbon dynamics

Vegetation carbon dynamics (VCD) regulates the functioning of terrestrial ecosystems that includes carbon capture (GPP), storage (NPP) and rate of storage (CUE) as the ratio of NPP to GPP. Here, VCD is shown in terms of the long-term trend in GPP and spatial variability in CUE (Fig. 4). Positive trend in GPP (greening) is estimated in IGP (Punjab, Haryana and UP) northwest (Rajasthan), west (Maharashtra), CI (MP) and SI (Karnataka). Negative trend in GPP (browning) is observed in IGP (Bihar, Jharkhand, West Bengal), CI (Chhattisgarh and Orissa), NE and SI (Tamil Nadu and Andhra Pradesh). The CUE variability in India in the last two decades (2000–2019) shows a specific pattern. For instance, the regions such as NW, IGP and some areas in CI exhibit small (<0.3) CUE, but higher CUE (0.45–0.6) in CI and SI. Croplands in the western areas of SI (0.6–0.75), and forests in the Himalaya and NE (0.6–0.9) show very high CUE. Therefore, greening is found in the regions of lower CUE and browning in higher CUE regions. This is a major concern as there is a need of proper planning and management to protect the green cover in these areas of higher CUE.

3.2.3. Vegetation types and CUE

Apart from climate variability, vegetation type also plays a key role in VCD (Yao et al., 2018). The CUE is a function of ecozones and vegetation types (De Lucia et al., 2007). The Indian landmass has rich and varied vegetated land such as forests, croplands, agroforestry and plantations, and each type with specific role in carbon sequestration (Murthy et al., 2013; Le Quéré et al., 2018). The major vegetation types in India are shown in Fig. S4 and are listed in Table S2. In the western Himalaya, savanna, woody savanna, shrublands and evergreen broadleaf forest exhibit very high CUE (0.75–0.9), as shown in Fig. 4. These regions are majorly alpine forests dominated by trees such as pine and oak. The evergreen broadleaf forests in the eastern Himalaya exhibit higher (>0.75) CUE. In CI, shrublands, savanna dominated by woody perennials and deciduous broadleaf forests also show higher (>0.6) CUE. The savannas, grasslands and croplands in CI and SI regions show CUE of 0.6 or higher. Croplands exhibit moderate (0.3–0.45) CUE in IGP,

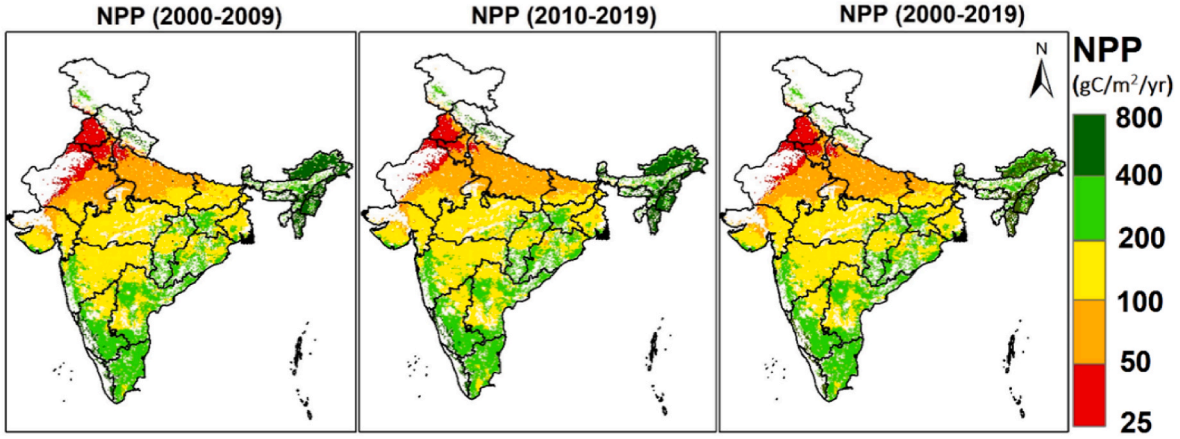

Fig. 2. Net Primary Productivity (NPP) averaged over the periods 2000–2009, 2010–2019 and 2000–2019.

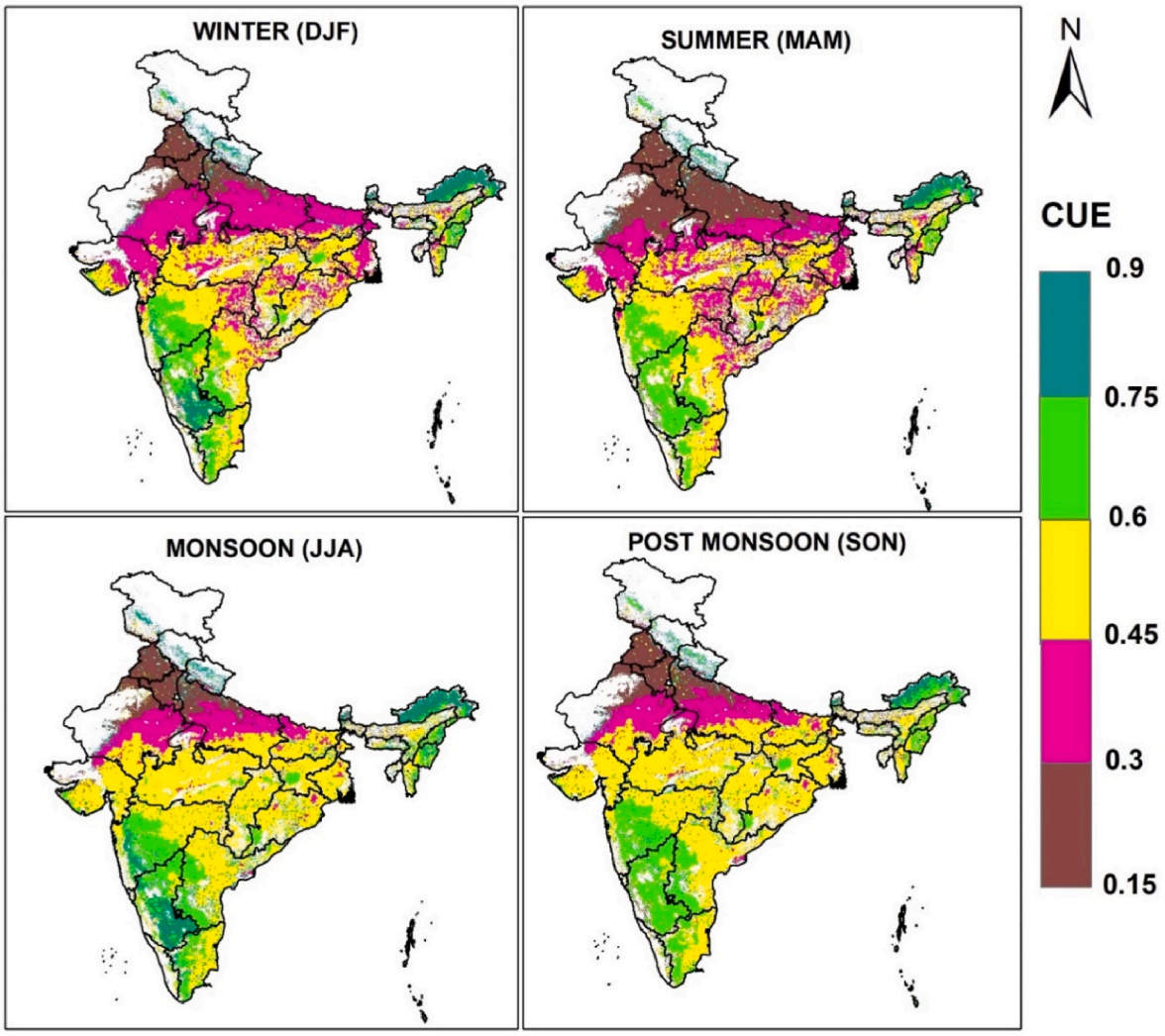

Fig. 3. The Carbon Use Efficiency (CUE) during winter (December, January and February), summer (March, April and May), monsoon (June, July and August) and post-monsoon (September, October and November) seasons averaged over the last 20 years (2000–2019).

CI and western coastal plains. The croplands in the western NW have low CUE (0.15–0.3). In general, forests exhibit higher CUE than that by croplands. Therefore, vegetation type is also a major factor in determining the CUE of ecosystems. VCD and CUE are ecosystem-specific parameters and they vary for different biomes and vegetation types (He et al., 2018; Gang et al., 2022). Henceforth, the selection of plant type is very important in reforestation, agroforestry and plantation activities, particularly for climate change mitigation measures.

3.3. CUE: variability, role of drivers and underlying mechanisms

3.3.1. Interannual variability

CUE is greatly affected by climate drivers such as T and P (He et al., 2018; Gang et al., 2022). The changing climate has highly influenced VCD with a reduction in NPP during the drought years (Bala et al., 2013; Gang et al., 2022). There are negative impacts of T extremes on cropland productivity (Lobell and Gourdji, 2012). Here, the interannual variability in CUE is explored in relation to its drivers in FPAR, SM, P, T and AOCC, as demonstrated in Fig. 5. The years 2003–2008, 2010, 2011, 2013 and 2014 with higher water availability (P and SM) and higher FPAR show higher CUE. However, CUE is lower in the years 2000–2002, 2009, 2012 and 2015 due to the reduction in water availability. The years of predominant warming such as 2002, 2009 and 2016 show the combined effect of limited P and high T, where the resulting low SM and FPAR lead to small CUE (warming induced moisture stress). In addition, these years also have higher AOCC, which negatively affect CUE. The water availability accompanied by cooling has led to higher CUE (moisture induced greening) in 2004, 2011 and 2013, as also found in other studies (e.g. Pérez-Girón et al., 2020, 2022).

3.3.2. Connection with drivers

PCA is carried out to understand the connection of CUE with its drivers, as shown in Fig. 5. Here, both UPCA and RPCA are performed with two PCs, namely PC1 and PC2 based on eigen values. PC1 is defined in UPCA by SM (0.84), P (0.66) and CUE (0.61) with positive correlation, whereas T (−0.83) and AOCC (−0.66) are correlated negatively with PC1. It shows that the water availability components in SM and P exhibit comparable variability as for CUE. This is expected as P drives SM and both have strong positive association with CUE. However, the negative correlation of T and AOCC with PC1 suggests that these factors have a detrimental effect on the variability of CUE and other variables in PC1. Due to the overwhelming negative influence of T and AOCC, FPAR (−0.38) shows a weak negative correlation with PC1. PC2 is largely determined by the variability of CUE (0.65), FPAR (0.81) and P (0.49); indicating that FPAR has a positive impact on the variability of CUE.

To better understand the relationship among the drivers and CUE, we used the varimax approach to rotate the PCs. In RPCA, it is observed that CUE (0.88), P (0.82) and SM (0.81) have a very strong positive

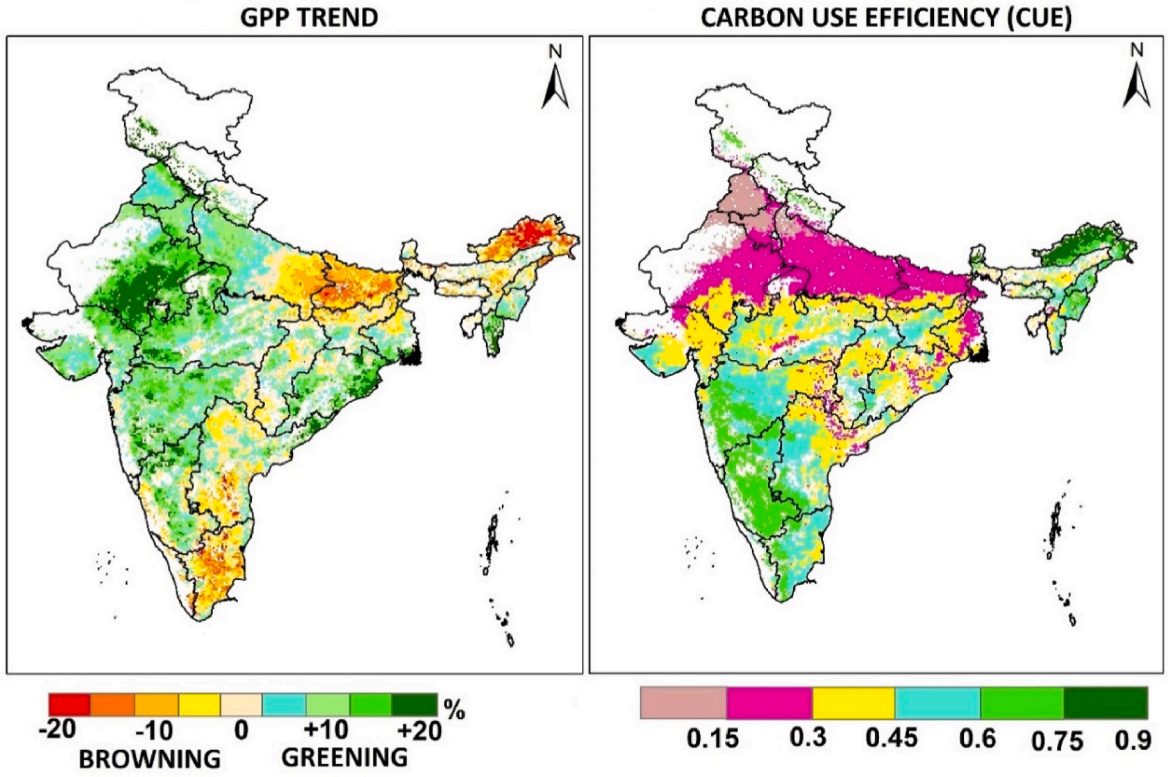

Fig. 4. Gross Primary Productivity (GPP) trend (decreasing– browning; increasing – greening). The ratio of NPP to GPP gives the Carbon Use Efficiency (CUE) for the period 2000–2019.

correlation with PC1, which indicates that these variables are highly connected among themselves. T (−0.41) has a negative correlation with PC1 as higher T will adversely affect CUE. PC2 is also distinguished by a strong positive correlation with FPAR (0.85), AOCC (0.84) and T (0.8). However, T (−0.41) also influences PC1 negatively as higher T will adversely affect SM, P and CUE. AOCC (−0.15) exhibits weak negative correlation with PC1, which suggests that it has a weak negative connection with CUE. Henceforth, PCA analysis demonstrates that both SM and P have strong positive association with CUE. This points out the close connection between carbon and water cycles in cropland dominated India.

3.3.3. Contribution and influence of drivers

CUE and VCD are regulated by the changes in terrestrial productivity, which is influenced by the spatial and temporal variability in drivers. SM (32.83%) is the most dominant driver of CUE in cropland dominated India; indicating a close link between carbon and water cycles. P (26.13%), FPAR (22.32%), and AOCC (16.47%) make significant contributions to CUE variability. The relative influence (positive/negative) of the drivers on the GPP trend and CUE is shown in Fig. 6. The positive influence of SM and T dominates over the negative influence of P and AOCC; leading to increase in productivity (greening) called moisture induced greening, which is observed in NW (Parida et al., 2020; Kashyap et al., 2022). In CI, positive influence of AOCC might be the reason for greening due the cooling effect there, which is also replicated by anthropogenic aerosol (brown haze) in this region (e.g. Kuttippurath and Raj, 2021). The enhanced productivity (greening) in IGP can be attributed to the anthropogenic intrusions such as the improvement in irrigation facilities, enhanced farm mechanisation and application of nitrogen-based fertilizers (Nayak et al., 2013; Ambika and Mishra., 2020). The negative influence of SM and T (warming induced moisture stress) is dominant over the positive influence of P, and that lead to reduced productivity (browning) in SI. The warming induced moisture stress is prevalent in this region, which is predominant in the areas of Tamil Nadu (e.g. Parida et al., 2020; Kashyap et al., 2022). In NE and eastern areas of IGP, large-scale anthropogenic activity (shifting cultivation and land abandoning) has led to green cover loss and browning. The NE region has severe consequences of human induced LULCC as the loss of vegetation cover drives extreme events such as fires and landslides in these ecologically fragile regions (Sannigrahi et al., 2020; Kashyap et al., 2021).

3.3.4. Causal discovery of drivers

The causal graphs/network are developed by considering various maximum time delay (T_{max}) or lag and significance threshold (ά) to understand the non-linear role of drivers in terrestrial VCD. As ά is increased from 0.1 to 0.05 and further to 0.01, the number of causal links diminishes and only the strong links remain. Also, the causal graphs at different T_{max} (lag) provide insights on the mechanisms influencing CUE and terrestrial VCD at different temporal scales ranging from T_{max} = 1–3 months, as shown in Fig. S5. Here, we have shown the causal graph for T_{max} = 4 (Fig. 7), where a number of causal structures are established at ά = 0.1. P does not have a direct causal link with CUE, but it drives SM that has a direct link with CUE with lag of 2 months. P also has a link with FPAR, which has a direct positive connection with CUE in a 1-month lag. FPAR is used as a proxy for photosynthesis and higher P would support more photosynthesis and faster carbon uptake (i.e. higher CUE). P has a negative link with T (lag = 1 month), which has direct negative link with CUE (lag = 2 months). Therefore, P affects CUE indirectly through other drivers. T has a strong negative link with FPAR, as photosynthetic activity responds well only to the optimum range of T, and therefore, CUE has a direct negative link with T. Furthermore, T has a negative link with SM, which has a direct positive link with CUE; explaining the negative link between T and CUE. AOCC also has a direct negative link with CUE, as biomass burning in extensive croplands and wild fires in forests release the stored carbon stocks captured by the vegetation and reduces CUE. Similar causal links are also observed for ά = 0.05 and for ά = 0.01.

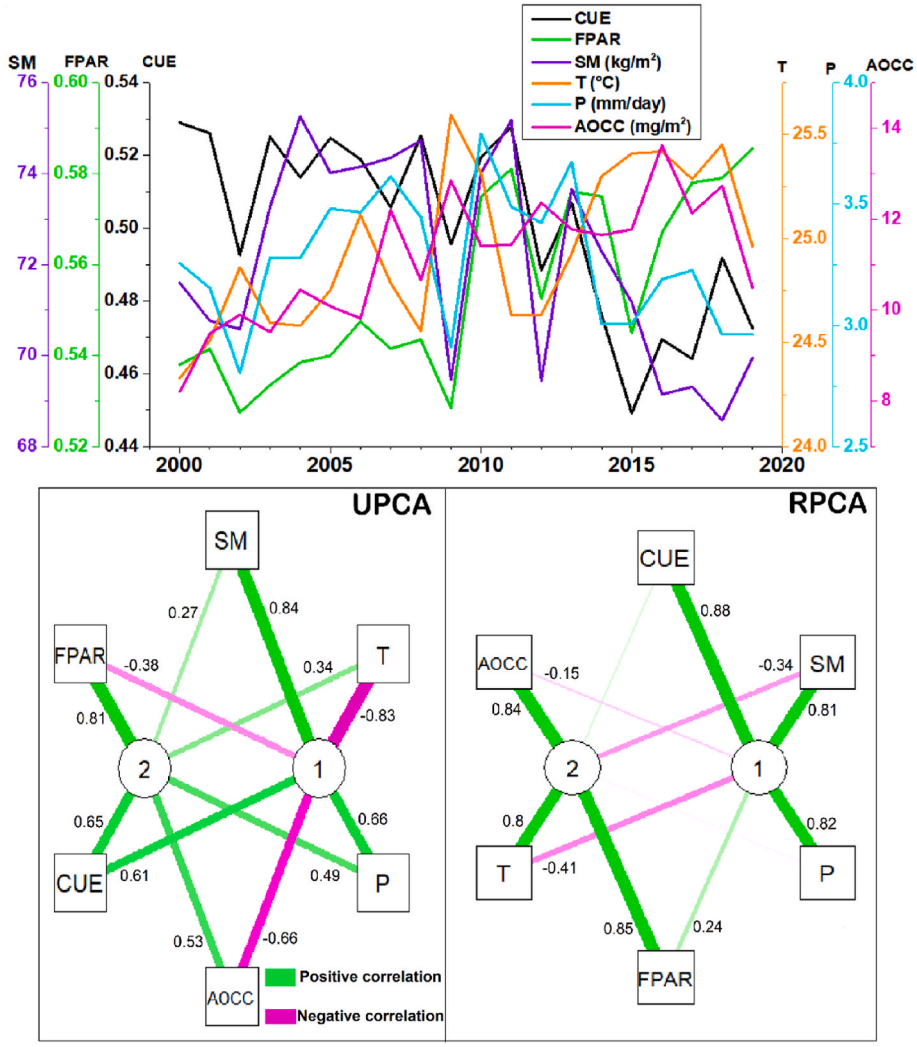

Fig. 5. Interannual variability in Carbon Use Efficiency (CUE) and its drivers– Fraction of Photosynthetically Active Radiation (FPAR), Precipitation (P), Temperature (T), Soil Moisture (SM) and Air Organic Carbon Content (AOCC) (top panel). The Principal Component Analysis (PCA) comprising of Unrotated PCA (UPCA) and Rotated PCA (RPCA) shows the links among CUE and its drivers. Here, the green and magenta lines represent positive and negative correlations, respectively. The thickness of the lines is a measure of the strength of the link represented in terms of correlation coefficients. (For interpretation of the references to colour in this figure legend, the reader is referred to the Web version of this article.)

4. Discussion

4.1. Background and our findings

India is second to China in global greening as revealed by the satellite-based leaf area index (LAI) analysis (Chen et al., 2019). However, quantification of this greening in terms of terrestrial VCD is still uncertain (Sarmah et al., 2021; Verma et al., 2022). Therefore, we utilised the MODIS data to understand the changes in terrestrial productivity for the last two decades. To find the carbon sequestration potential of vegetated land, CUE is estimated, for the first time for India.

Regarding the productivity, Singh et al. (2011) utilised satellite data and model results, and found a positive trend of 8.5%/dec in NPP for India during the period 1981–2000. Another study by Nayak et al. (2013), by using model results, showed that the increase in agricultural production is the major reason for enhanced NPP in India during the period 1981–2006. Bala et al. (2013) reported about 4%/dec increase of NPP in India based on the AVHRR satellite data for the period 1982–2006. Our analysis also shows that there is about 13% increase in NPP during the study period (2000–2019). In addition, Bala et al. (2013) showed that the seasonal cycle of terrestrial productivity is strongly influenced by SM in India. Kashyap et al. (2022) also revealed that SM is the dominant driver of photosynthetic trend in India during the last two decades. The carbon-water cycle interactions in India is complex and exhibit high regional variability owing to the conventional irrigation pattern in the croplands (Verma et al., 2022). Our analyses show that SM has a dominant role in driving VCD and thus, expose a strong link between carbon and water cycle in India. However, Sarmah et al. (2021) found that there is a mismatch between the greening trends and terrestrial carbon uptake in south Asia. The greening is largely observed in the croplands, which has limited carbon uptake potential. This is also reciprocated in our study as the high CUE regions are browning. This is a big concern for the terrestrial VCD with implications for anthropogenic climate change.

4.2. Novelty and wider implications

Most studies have relied on either correlation (Bala et al., 2013) or partial correlation (Sarmah et al., 2021) for finding the role of potential drivers in the variability of terrestrial productivity. A recent study by Verma et al. (2022) utilised causal discovery to find the drivers of GPP. However, there were limited number of drivers with known influence. Our analysis is not centred around the causal approach, but we utilise the method to examine the robustness of our results derived using various statistical techniques such as the correlation analysis, MLR and PCA. Our study provides new insights on the rate of carbon allocation and conversion to new biomass in ecosystems. Furthermore, it brings into light the ecologically vulnerable regions (NE, eastern IGP and some areas in SI), which requires immediate attention to increase the green cover for maintaining balance in the terrestrial carbon cycle, and also to mitigate carbon-induced climate change. Since India has various vegetation types, our study would also serve as a reference for quantification

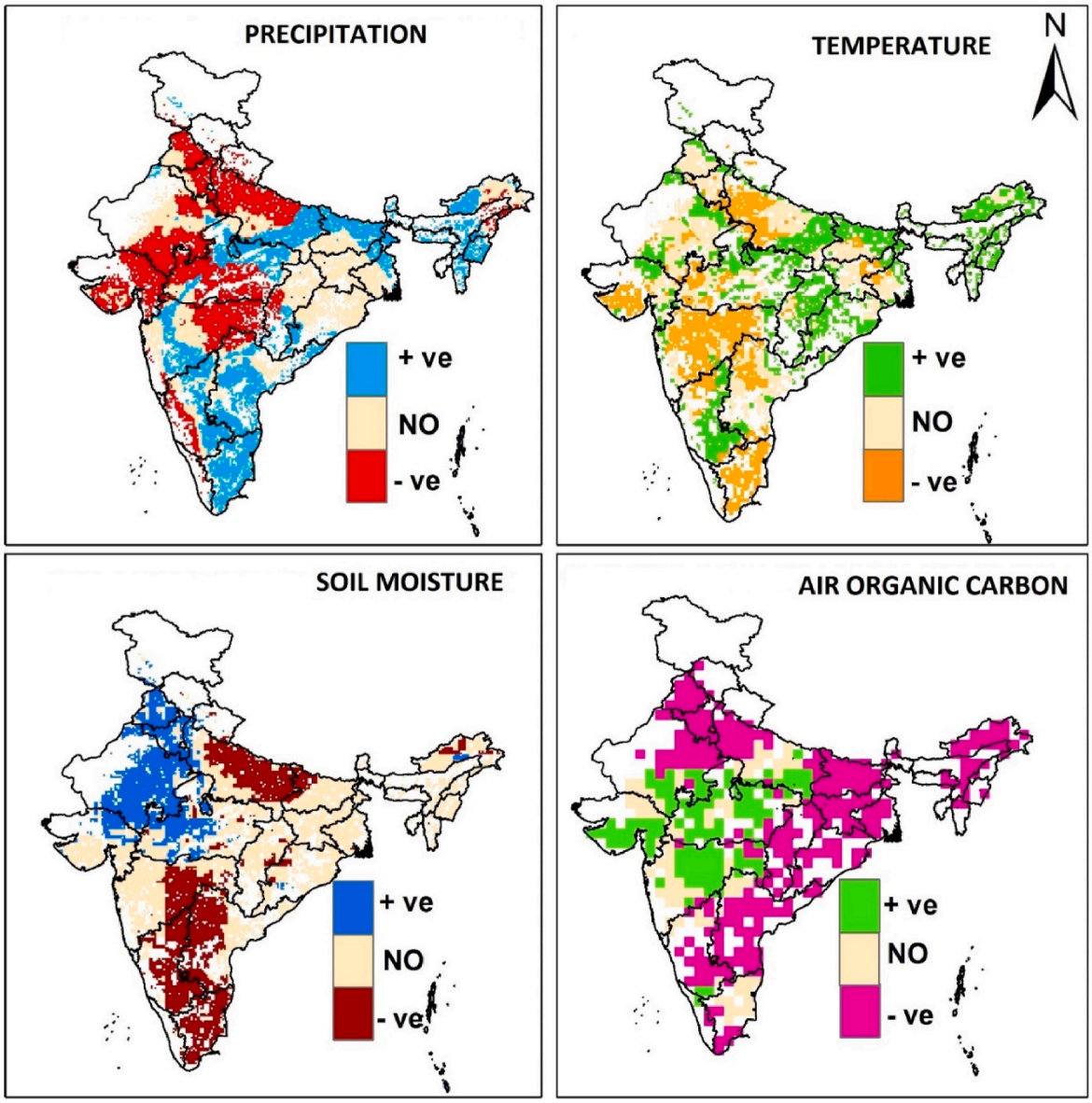

Fig. 6. Relative influence (negative/positive) of the spatial trend in climate drivers– precipitation (drying/showering), temperature (cooling/warming), soil moisture (drying/moistening), and air organic carbon content (high/low) on the productivity trend (browning/greening) and Carbon Use Efficiency (CUE) over the period 2000–2019.

and understanding the mechanisms influencing VCD at regional and global scales. Additionally, our analyses would enhance the performance of Earth System models by providing better model input for carbon fluxes between land and atmosphere. The balance in the terrestrial carbon cycle is key to achieve ambient atmospheric and environmental conditions. Weakening of efficient vegetation carbon sinks is a great concern for sustainability, global warming and climate change. Knowledge about the country-wide terrestrial VCD is very important to draft policies for mitigating climate change impacts on food production and to achieve sustainable development goals (SDGs).

4.3. Constraints

Improved spatial resolution of the datasets would give more detailed information on terrestrial VCD. This study assumes the seasonal variability in NPP to be the same as that of GPP for estimating CUE as there are no seasonal datasets for NPP. The contribution of drivers estimated here is the "relative contribution" where the sum of contribution of all drivers is 100%. As there can be other drives, this assessment does not claim exact contribution of any driver in regulating VCD. Since the MODIS data are available from 2000 onwards, and the years 2020 and 2021 have the influence of COVID-induced lockdown (Kashyap et al., 2023), the period 2000–2019 is considered in our analysis. Ground-based measurements of productivity might provide better results, but those are not available for the Indian region to assess VCD. Therefore, the above -mentioned limitations could influence the uncertainty of the estimates.

5. Conclusions

The vegetation carbon dynamics (VCD) regulates functioning of terrestrial ecosystems, as it includes carbon capture (GPP), storage (NPP) and rate of storage (CUE). Here, we have utilised PCA, MLR and causal discovery to examine the key drivers of CUE variability in India for the period 2000–2019. Water availability (SM and P) promotes higher CUE, but higher T and AOCC reduce CUE. There is an increase in

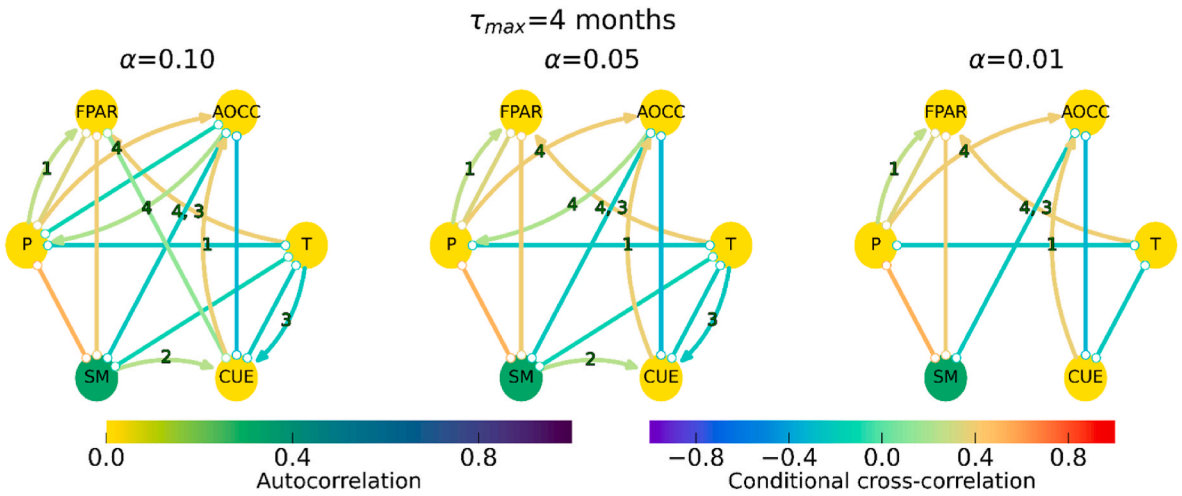

Fig. 7. Causal graphs representing the links for relation of Carbon Use Efficiency (CUE) with its drivers, and interrelationship among Fraction of Photosynthetically Active Radiation (FPAR), Precipitation (P), Temperature (T) Soil Moisture (SM) and Air Organic Carbon Content (AOCC). Here, the maximum time delay is T_{max} and significance threshold is ά.

productivity (greening) in regions of lower CUE in NW (moisture induced greening) and IGP (irrigation induced agricultural boom). However, a reduced productivity (browning) is found in regions of higher CUE such as NE, lower IGP (deforestation and extreme events) and SI (warming induced moisture stress). Apart from climate drivers, anthropogenic intrusions (e.g. land use change, irrigation, farm mechanisation and pollution) also play a role in regulating VCD. Since browning is found in regions of higher CUE, it is a major concern as it indicates weakening of efficient terrestrial carbon sinks. Thus, there is a need of proper planning to protect the green cover in the areas of higher CUE.

This study, therefore, recommends preservation of green cover for maintaining balance in the terrestrial carbon cycle. The preservation of indigenous green cover and afforestation, particularly in the regions of higher vegetation CUE, is very important as it would reduce the carbon footprints in the world of global warming, rising population and high pollution. Our analysis provides new insights on the rate of carbon allocation and help to accurately quantify the ability of vegetation to convert carbon to new biomass in ecosystems. Accurate quantification of CUE for different ecozones and vegetation types would enhance the performance of Earth System Models by providing better input for land-atmosphere interactions. These findings would enable us to counter the challenges of food security, global warming, climate change, and attain sustainability by drafting and implementing relevant policies.

Credit authors statement

RK: Conceptualization, Methodology, Data Analyses, Visualization, Validation, Software, Writing–original draft. **JK:** Conceptualization, Methodology, Visualization, Supervision, review and editing of the original draft. **PK**: Data Analyses, Visualization and Software.

Declaration of competing interest

The authors declare that they have no known competing financial interests or personal relationships that could have appeared to influence the work reported in this paper.

Data availability

All data are publicly available, but can also be made available on request. All data are listed in Table 1.

Acknowledgements

We thank the Director, Indian Institute of Technology Kharagpur (IIT Kgp), Chairman of CORAL IIT Kgp and the Ministry of Education (MoE) for facilitating the study. RK acknowledges the support from Prime Minister's Research Fellowship (PMRF), MoE and PK acknowledges the support from MoE, IIT KGP. We thank the NASA's LPDAAC team for providing the MODIS landcover, NDVI, GPP and NPP products. Giovanni's online data system developed and maintained by the NASA GES DISC for providing the GPM level–3 precipitation data, GLDAS for providing temperature and soil moisture content datasets and MERRA 2 air organic carbon content datasets. We thank the anonymous reviewers and the editor for their comments to improve the quality of this study.

Appendix A. Supplementary data

Supplementary data to this article can be found online at https://doi.org/10.1016/j.jenvman.2023.117655.

References

Ambika, A.K., Mishra, V., 2020. Substantial decline in atmospheric aridity due to irrigation in India. Environ. Res. Lett. 15 (12), 124060 https://doi.org/10.1088/1748-9326/abc8bc.

Bala, G., Joshi, J., Chaturvedi, R.K., Gangamani, H.V., Hashimoto, H., Nemani, R., 2013. Trends and variability of AVHRR– derived NPP in India. Rem. Sens. 5 (2), 810–829. https://doi.org/10.3390/rs5020810.

Ballantyne, A.Á., Alden, C.Á., Miller, J.Á., Tans, P.Á., White, J.W.C., 2012. Increase in observed net carbon dioxide uptake by land and oceans during the past 50 years. Nature 488 (7409), 70–72. https://doi.org/10.1038/nature11299.

Campbell, J.E., Berry, J.A., Seibt, U., Smith, S.J., Montzka, S.A., Launois, T., Belviso, et al., 2017. Large historical growth in global terrestrial gross primary production. Nature 544 (7648), 84–87. https://doi.org/10.1038/nature22030.

Chen, C., Park, T., Wang, X., Piao, S., Xu, B., Chaturvedi, R.K., et al., 2019. China and India lead in greening of the world through land–use management. Nat. Sustain. 2 (2), 122–129. https://doi.org/10.1038/s41893-019-.

De Lucia, E.H., Drake, J.E., Thomas, R.B., Gonzalez-Meler M I Q U E L., 2007. Forest carbon use efficiency: is respiration a constant fraction of gross primary production? Global Change Biol. 13 (6), 1157–1167. https://doi.org/10.1111/j.1365-2486.2007.01365.x.

Gahlot, S., Shu, S., Jain, A.K., Baidya Roy, S., 2017. Estimating trends and variation of net biome productivity in India for 1980–2012 using a land surface model. Geophys. Res. Lett. 44 (22), 11–573. https://doi.org/10.1002/2017GL075777.

Gang, C., Wang, Z., You, Y., Liu, Y., Xu, R., Bian, Z., et al., 2022. Divergent responses of terrestrial carbon use efficiency to climate variation from 2000 to 2018. Global Planet. Change 208, 103709. https://doi.org/10.1016/j.gloplacha.2021.103709.

Gao, T., Yu, J.Y., Paek, H., 2017. Impacts of four northern–hemisphere teleconnection patterns on atmospheric circulations over Eurasia and the Pacific. Theor. Appl. Climatol. 129 (3), 815–831. https://doi.org/10.1007/s00704-016-1801-2.

Garbulsky, M.F., Filella, I., Verger, A., Peñuelas, J., 2014. Photosynthetic light use efficiency from satellite sensors: from global to Mediterranean vegetation. Environ. Exp. Bot. 103, 3–11. https://doi.org/10.1016/j.envexpbot.2013.10.009.

He, Y., Piao, S., Li, X., Chen, A., Qin, D., 2018. Global patterns of vegetation carbon use efficiency and their climate drivers deduced from MODIS satellite data and process–based models. Agric. For. Meteorol. 256, 150–158. https://doi.org/10.1016/j.agrformet.2018.03.009.

IPCC, 2019. Climate Change and Land: an IPCC Special Report on Climate Change, Desertification, Land Degradation, Sustainable Land Management, Food Security, and Greenhouse Gas Fluxes in Terrestrial Ecosystems.

Kashyap, R., Pandey, A.C., Kuttippurath, J., 2022. Photosynthetic trends in India derived from remote sensing measurements during 2000–2019: vegetation dynamics and key climate drivers. Geocarto Int. 1–17. https://doi.org/10.1080/10106049.2022.2060325.

Kashyap, R., Pandey, A.C., Parida, B.R., 2021. Spatio–temporal variability of monsoon precipitation and their effect on precipitation triggered landslides in relation to relief in Himalayas. Spat Inf Res 29 (6), 857–869. https://doi.org/10.1007/s41324-021-00392-8.

Kashyap, R., Kuttippurath, J., Patel, V.K., 2023. Improved air quality leads to enhanced vegetation growth during the COVID–19 lockdown in India. Appl. Geogr., 102869 https://doi.org/10.1016/j.apgeog.2022.102869.

Krich, C., Runge, J., Miralles, D.G., Migliavacca, M., Perez–Priego, O., El–Madany, T., Mahecha, M.D., et al., 2020. Estimating causal networks in biosphere–atmosphere interaction with the PCMCI approach. Biogeosciences 17 (4), 1033–1061. https://doi.org/10.5194/bg-17-1033-2020.

Kumar, P., Kuttippurath, J., Mitra, A., 2022. Causal discovery of drivers of surface ozone variability in Antarctica using a deep learning algorithm. Environ SciProcess Impacts 24 (3), 447–459. https://doi.org/10.1039/D1EM00383F.

Kuttippurath, J., Murasingh, S., Stott, P.A., Sarojini, B.B., Jha, M.K., Kumar, P., et al., 2021. Observed rainfall changes in the past century (1901–2019) over the wettest place on Earth. Environ. Res. Lett. 16 (2), 024018 https://doi.org/10.1088/1748-9326/abcf78.

Kuttippurath, J., Nair, P.J., 2017. The signs of Antarctic ozone hole recovery. Sci. Rep. 7 (1), 1–8. https://doi.org/10.1038/s41598-017-00722-7.

Kuttippurath, J., Raj, S., 2021. Two decades of aerosol observations by AATSR, MISR, MODIS and MERRA–2 over India and Indian Ocean. Remote Sens. Environ. 257, 112363 https://doi.org/10.1016/j.rse.2021.112363.

Le Quéré, C., Andrew, R.M., Friedlingstein, P., Sitch, S., Hauck, J., Pongratz, J., Arneth, A., et al., 2018. Global carbon budget 2018. Earth Syst. Sci. Data 10 (4), 2141–2194. https://doi.org/10.18160/GCP-2018.

Lim, Y.K., 2015. The East atlantic/west Russia (EA/WR) teleconnection in the north–atlantic: climate impact and relation to rossby wave propagation. Clim. Dynam. 44, 3211–3222. https://doi.org/10.1007/s00382-014-2381-4.

Liu, S., Cheng, F., Dong, S., Zhao, H., Hou, X., Wu, X., 2017. Spatiotemporal dynamics of grassland aboveground biomass on the Qinghai–Tibet Plateau based on validated MODIS NDVI. Sci. Rep. 7 (1), 1–10. https://doi.org/10.1038/s41598-017-04038-4.

Liu, Y., Liu, Y., Wang, W., 2019. Inter–comparison of satellite–retrieved and Global Land Data Assimilation System–simulated soil moisture datasets for global drought analysis. Remote Sens. Environ. 220, 1–18. https://doi.org/10.1016/j.rse.2018.10.026.

Lobell, D.B., Gourdji, S.M., 2012. The influence of climate change on global crop productivity. Plant Physiol. 160 (4), 1686–1697. https://doi.org/10.1104/pp.112.208298.

Mezzina, B., Garcia–Serrano, J., Blade, I., Kucharski, F., 2020. Dynamics of the ENSO teleconnection and NAO variability in the North Atlantic–European late winter. J. Clim. 33, 907–923. https://doi.org/10.1175/JCLI-D-19-0192.1.

Migliavacca, M., Musavi, T., Mahecha, M.D., Nelson, J.A., Knauer, J., Baldocchi, D.D., et al., 2021. The three major axes of terrestrial ecosystem function. Nature 598 (7881), 468–472. https://doi.org/10.1038/s41586-021-03939-9.

Muñoz, E., Poveda, G., Arbeláez, M.P., Vélez, I.D., 2021. Spatiotemporal dynamics of dengue in Colombia in relation to the combined effects of local climate and ENSO. Acta Trop. 224, 106136 https://doi.org/10.1016/j.actatropica.2021.106136.

Murthy, I.K., Gupta, M., Tomar, S., Munsi, M., Tiwari, R., Hegde, G.T., Ravindranath, N. H., 2013. Carbon sequestration potential of agroforestry systems in India. J. Earth Sci. Climatic Change 4 (1), 1–7. https://doi.org/10.4172/2157-7617.1000131.

Nayak, R.K., Patel, N.R., Dadhwal, V.K., 2013. Inter-annual variability and climate control of terrestrial net primary productivity over India. Int. J. Climatol. 33 (1), 132–142. https://doi.org/10.1002/joc.3414.

Nemani, R.R., Keeling, C.D., Hashimoto, H., Jolly, W.M., Piper, S.C., Tucker, C.J., et al., 2003. Climate-driven increases in global terrestrial net primary production from 1982 to 1999. Science 300 (5625), 1560–1563. https://doi.org/10.1126/science.1082750.

Newbold, T., Tittensor, D.P., Harfoot, M.B., Scharlemann, J.P., Purves, D.W., 2020. Non–linear changes in modelled terrestrial ecosystems subjected to perturbations. Sci. Rep. 10 (1), 1–10. https://doi.org/10.1038/s41598-020-70960-9.

Parida, B.R., Pandey, A.C., Patel, N.R., 2020. Greening and browning trends of vegetation in India and their responses to climatic and non–climatic drivers. Climate 8 (8), 92. https://doi.org/10.3390/cli8080092.

Pérez-Girón, J.C., Alvarez-Alvarez, P., Díaz-Varela, E.R., Lopes, D.M.M., 2020. Influence of climate variations on primary production indicators and on the resilience of forest ecosystems in a future scenario of climate change: application to sweet chestnut agroforestry systems in the Iberian Peninsula. Ecol. Indicat. 113, 106199 https://doi.org/10.1016/j.ecolind.2020.106199.

Pérez-Girón, J.C., Díaz-Varela, E.R., Álvarez-Álvarez, P., 2022. Climate-driven variations in productivity reveal adaptive strategies in Iberian cork oak agroforestry systems. Ecosystems 9, 100008. https://doi.org/10.1016/j.fecs.2022.100008.

Piao, S., Wang, X., Park, T., Chen, C., Lian, X.U., He, Y., Bjerke, J.W., Myeni, R.B., et al., 2020. Characteristics, drivers and feedbacks of global greening. Nat. Rev. Earth Environ. 1 (1), 14–27. https://doi.org/10.1038/s43017-019-0001-x.

Roxburgh, S.H., Berry, S.L., Buckley, T.N., Barnes, B., Roderick, M.L., 2005. What is NPP? Inconsistent accounting of respiratory fluxes in the definition of net primary production. Funct. Ecol. 19 (3), 378–382. https://www.jstor.org/stable/3599129.

Runge, J., Bathiany, S., Bollt, E., Camps–Valls, G., Coumou, D., Deyle, E., Zscheischler, J., et al., 2019. Inferring causation from time series in Earth system sciences. Nat. Commun. 10 (1), 1–13. https://doi.org/10.1038/s41467-019-10105-3.

Running, S., Mu, Q., Zhao, M., 2015. MOD17A2H MODIS/Terra Gross Primary Productivity 8– Day L4 Global 500m SIN Grid V006. NASA EOSDIS L. Process. DAAC.

Sannigrahi, S., Pilla, F., Basu, B., Basu, A.S., Sarkar, K., Chakraborti, S., et al., 2020. Examining the effects of forest fire on terrestrial carbon emission and ecosystem production in India using remote sensing approaches. Sci. Total Environ. 725, 138331 https://doi.org/10.1016/j.scitotenv.2020.138331.

Sarmah, S., Singha, M., Wang, J., Dong, J., Burman, P.K.D., Goswami, S., Ge, Y., Ilyas, S., Niu, S., 2021. Mismatches between vegetation greening and primary productivity trends in South Asia-A satellite evidence. Int. J. Appl. Earth Obs. Geoinf. 104, 102561 https://doi.org/10.1016/j.jag.2021.102561.

Shikwambana, L., 2019. Long-term observation of global black carbon, air organic carbon and smoke using CALIPSO and MERRA– 2 data. Remote Sens. Lett. 10 (4), 373–380. https://doi.org/10.1080/2150704X.2018.1557789.

Singh, A., Abbhishek, K., Kuttippurath, J., Raj, S., Mallick, N., Chander, G., Dixit, S., 2022. Decadal variations in CO2 during agricultural seasons in India and role of management as sustainable approach. Environ. Technol. Innovat. 27, 102498 https://doi.org/10.1016/j.eti.2022.102498.

Singh, R.P., Rovshan, S., Goroshi, S.K., Panigrahy, S., Parihar, J.S., 2011. Spatial and temporal variability of net primary productivity (NPP) over terrestrial biosphere of India using NOAA–AVHRR based GloPEM model. J. Ind. Soc. Remote Sens. 39, 345–353. https://doi.org/10.1007/s12524-011-0123-1.

Spensberger, C., Reeder, M.J., Spengler, T., Patterson, M., 2020. The connection between the Southern Annular Mode and a feature–based perspective on Southern Hemisphere midlatitude winter variability. J. Clim. 33, 115–129. https://doi.org/10.1175/JCLI-D-19-0224.1.

Turner, D.P., Ritts, W.D., Cohen, W.B., Gower, S.T., Running, S.W., Zhao, M., et al., 2006. Evaluation of MODIS NPP and GPP products across multiple biomes. Remote Sens. Environ. 102 (3– 4), 282–292. https://doi.org/10.1016/j.rse.2006.02.017.

Verma, A., Chandel, V., Ghosh, S., 2022. Climate drivers of the variations of vegetation productivity in India. Environ. Res. Lett. 17 (8), 084023 https://doi.org/10.1088/1748-9326/ac7c7f.

Wang, L., Li, X., Chen, Y., Yang, K., Chen, D., Zhou, J., et al., 2016. Validation of the global land data assimilation system based on measurements of soil temperature profiles. Agric. For. Meteorol. 218, 288–297. https://doi.org/10.1016/j.agrformet.2016.01.003.

Wang, L., Zhu, H., Lin, A., Zou, L., Qin, W., Du, Q., 2017. Evaluation of the latest MODIS GPP products across multiple biomes using global eddy covariance flux data. Rem. Sens. 9 (5), 418. https://doi.org/10.3390/rs9050418.

Xia, Y., Hao, Z., Shi, C., Li, Y., Meng, J., Xu, T., et al., 2019. Regional and global land data assimilation systems: innovations, challenges, and prospects. J. Meteorol. Res. 33 (2), 159–189. https://doi.org/10.1007/s13351-019-8172-4.

Xu, R., Tian, F., Yang, L., Hu, H., Lu, H., Hou, A., 2017. Ground validation of GPM IMERG and TRMM 3B42V7 rainfall products over southern Tibetan Plateau based on a high-density rain gauge network. J. Geophys. Res. Atmos. 122 (2), 910–924. https://doi.org/10.1002/2016JD025418.

Yao, Y., Wang, X., Li, Y., Wang, T., Shen, M., Du, M., He, H., Li, Y., Piao, S., et al., 2018. Spatiotemporal pattern of gross primary productivity and its covariation with climate in China over the last thirty years. Global Change Biol. 24 (1), 184–196. https://doi.org/10.1111/gcb.13830.